Experimental Mechanics (2016) 56:569–581
DOI 10.1007/s11340-015-0071-8

Near Field Underwater Explosion Response of Polyurea Coated Composite Plates

J. LeBlanc[1] · C. Shillings[2] · E. Gauch[1] · F. Livolsi[1] · A. Shukla[2]

Received: 1 April 2015 / Accepted: 1 July 2015 / Published online: 30 July 2015

Abstract An experimental study with corresponding numerical simulations has been conducted to evaluate the response of E-Glass / Epoxy composite plates, including polyurea coating effects, subjected to near field underwater explosion (UNDEX) loading. Experiments are performed in a water filled blast tank in which the including transient plate response during the UNDEX loading is measured utilizing high speed photography coupled with Digital Image Correlation. The experimental results show that the transient response of the plate is improved through the use of a thicker plate or through the application of a polyurea coating, although there is a weight penalty associated with the additional material which should be considered. Corresponding computational models of the experiments have been conducted with the commercial finite element code LS-Dyna. The simulations are shown to have a high level of correlation to the experimental data.

Keywords Composite materials · UNDEX loading · Polyurea coatings · Computational modeling · Digital image correlation

Introduction

Within the naval community there is an interest in constructing new vehicles and structures from composite materials. The advantages of these advanced material systems include high strength to weight ratios, lighter structural components, and overall reduced maintenance costs. However, when structures manufactured from these materials are employed in military applications they must also be designed in a manner such that they will be able to survive an underwater explosion (UNDEX) event. The static response of composite materials is well understood while there is less of an understanding in terms of what happens to the same composite material when subjected to high loading rates. This typically results in composite structures being conservatively designed with large safety factors. Due to these large safety factors the structures are often over designed, thus not fully utilizing the high strength to weight ratio afforded by composite materials. In the current study, the response of E-Glass / Epoxy composite plates, with and without polyurea coatings, subjected to near field underwater explosion (UNDEX) loading has been analyzed. Two parameters are investigated in the study: (1) Effect of the thickness of the baseline uncoated plate, and (2) Effect of coating the back-face of the plate (side opposite of explosive charge) with polyurea. The investigation consists of experiments performed in an underwater blast tank including the use of Digital Image Correlation (DIC) to capture the transient response of the plates. Corresponding computational simulations were performed with the commercial finite element code LS-Dyna.

When a submerged structure is exposed to an underwater explosion, it undergoes a complex and highly transient loading condition including high peak pressures and spherical wave fronts. When explosions occur at sufficiently large standoff distances from a structure, the shock fronts are nearly planar and act over the entire structure in a nearly uniform manner. This loading results in structural responses consisting primarily of flexure with large center-point deflections. However, there tends to be low levels of material damage (primarily interlaminar delaminations) and plate perforations / ruptures are minimal. In the absence of plate rupture, the shock wave is

✉ J. LeBlanc
james.m.leblanc@navy.mil

[1] Naval Undersea Warfare Center (Division Newport), 1176 Howell Street, Newport, RI 02841, USA

[2] University of Rhode Island, 92 Upper College Road, Kingston, RI 02881, USA

almost fully reflected away from the structure, shielding any occupants / internal equipment from the effects of the high pressure waves. Conversely, when an explosion occurs directly on, or very close to, the surface of a structure, the loading area is limited to the vicinity of the detonation itself. The result is highly localized pressure loadings and the structure sustains higher amounts of damage, oftentimes including plate penetration / complete rupture. Upon rupture of the plate the pressure waves enter the structure, subsequently exposing any occupants to the adverse effects of high pressure gases as well as any shrapnel which may become dislodged from the blast area.

Studies on composite materials subjected to high loading rates have utilized both experimental and computational techniques. Work by Latourte et al. [1] utilized a scaled fluid structure method [2] to study the failure modes and damage mechanisms in both monolithic and sandwich plates subjected to underwater impulsive loads. Schiffer and Tagarelli [3] have compared the response of glass and carbon reinforced composites and found that the glass reinforced plates had larger blast resistance than the carbon plates due to their higher tensile ductility. Avachat and Zhou [4] studied the effects of underwater shock loading on filament wound and sandwich composite cylinder and found that while both constructions exhibited similar damage mechanisms, including delamination, fiber failure and matrix cracking, the sandwich structure had overall better performance than a monolithic cylinder with similar mass. The same authors [5] also utilized an Underwater Shock Loading Simulator combined with digital image correlation to show that for sandwich constructions lower density cores yield higher blast performance than high density cores due to their larger core compression capability. LeBlanc and Shukla [6, 7] have studied the response of flat and curved composite plates to far field underwater explosive loading through experimental and computational methods. Franz et al. [8] and Mouritz et al. [9] studied the effects of an underwater explosion at different standoff distances on a glass composite laminate. Dear and Brown [10] have conducted a detailed study on the damage mechanisms and energy absorption in composite plates when subjected to impact loading.

In recent years, the use of polyurea materials to enhance the failure resistance of structures subjected to explosive loading has become a topic of interest. Polyurea is a synthetic, high strength / high elongation coating that is typically spray cast onto existing structures to increase their performance under shock and ballistic loading events such as those of a bomb blast. The armed forces have begun to investigate the suitability of these materials for use on military and naval vehicles such as Humvees, troop carriers and ship hulls, Hodge [11]. Research efforts have recently studied the effectiveness of polyurea when used with composite materials. LeBlanc et al. [12, 13] showed that the transient response of UNDEX loaded composite plates is dependent upon both coating thickness as well as location. Tekalur et al. [14] investigated the response of E-Glass composites coated with polyurea subjected to air blast loading. This study indicated that the polyurea coating reduced the transient deflections and post mortem damage levels as compared to the uncoated material. Gardner et al. [15] studied the effect of location of the polyurea in relation to the foam core in sandwich composites. It was observed that when a layer of polyurea is placed between the foam core and the back-face of the sandwich the blast resistance is improved, while conversely if the polyurea is placed between the front face and the foam core the performance is degraded. Furthermore, effects of polyurea coatings have been studied through the use of computational simulations. Amirkhizi et al. [16] have developed a visco-elastic constitutive material model that describes the behavior of polyurea materials under a broad range of strain rates, and includes pressure and temperature effects. Amini et al. [17, 18] used LS-DYNA to simulate impact / impulsive loading experiments of polyurea coated steel plates.

Materials

In the current study, E-Glass Epoxy bi-axial laminate composite plates, with and without polyurea coatings are studied. The following section details the materials utilized in the investigation.

Composite

The composite material used in this investigation is Cyply® 1002, a reinforced plastic manufactured by Cytec Engineered Materials. The material is a cured epoxy composite which utilizes a non-woven, parallel fiber construction with continuous E-Glass filaments. A cross-ply construction has been utilized in this study that has alternating plies of 0° and 90° with each ply having a thickness of 0.254 mm (0.01 in.). The cured material has an areal weight of 0.46 kg/m^2 (0.85 lb/yd^2) per ply (0.254 mm) and a specific gravity of 1.85. The resin content is 36±3 %. Two plate thicknesses, 0.762 mm and 1.524 mm, have been utilized in the study. The 0.762 mm plates have 3 lamina of alternating 0/90 plies such that the laminate schedule is [0/90/0] while the 1.524 mm plate has a schedule of [0/90/0/90/0/90]. The properties for a single unidirectional ply of the material are provided in Table 1.

Polyurea

The composite laminate serves as the baseline substrate to which the polyurea coatings are applied. In the current study the 0.762 mm composite plate has been coated with a polyurea coating having a thickness of 0.762 mm. This results in a plate with a combined thickness of 1.524 mm, equal to that of the thicker composite plate. The coating is applied to the back side of the plate after manufacturing and is not integrated into the

Table 1 Cyply 1002 - mechanical properties (Uni-directional)

	MPa
Tensile Modulus (0°)	39.3e3
Tensile Modulus (90°)	9.65e3
Tensile Strength (0°)	965
Tensile Strength (90°)	20
Compressive Strength (0°)	883
Compressive Strength (90°)	193

composite itself. This construction is chosen to represent what would typically be found in a real world application where structures are retrofitted (spray coated) with this material as opposed to being incorporated into the original design. The polyurea is sprayed onto the plates and then post cured for 48 h at a temperature of 160 °F.

The polyurea material used is Dragonshield-BC available from Specialty Products, Inc. of Lakewood, WA. This is a 2 part material that can be spray cast to a wide range of surfaces and materials. The polyurea has been characterized in both tension and compression for strain rates from 0.01 to 2000 s^{-1}. Characterization up to 100 s^{-1} was performed using standard material testing machine whereas a split Hopkinson pressure bar was used to characterize the response of the material at 2000 s^{-1}. The response of the material at 2000 s^{-1} was only characterized in compression and is assumed to be similar in tension. At the lower strain rates unique tests were conducted for both tension and compression. The full material characterization is shown in Fig. 1. From this figure it is seen that the material exhibits strong strain rate dependence and becomes stiffer with increasing loading rate. Furthermore the material displays a stiffening effect in compression above 300 % whereas in tension the response exhibits a stress plateau like behavior.

A summary of the plate thicknesses and areal weights is provided in Table 2, and a schematic of the laminate designs are shown in Fig. 2.

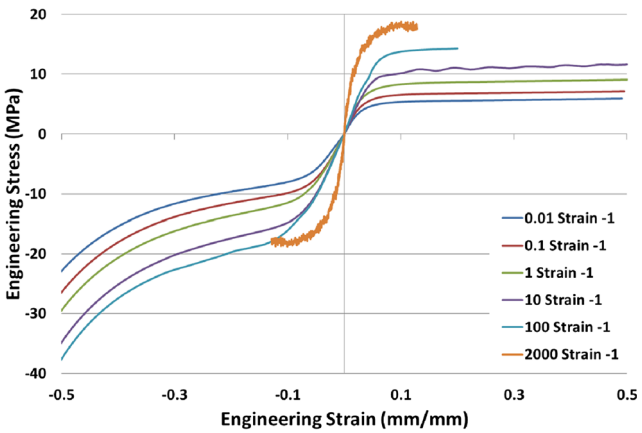

Fig. 1 Dragon shield BC Polyurea stress–strain behavior

Table 2 Thickness and areal weight of laminates

	Thickness, mm (in)	Areal Weight, kg/m^2 (oz/yd^2)
Thin Baseline Laminate	0.762 (0.03)	1.45 (42.7)
Thick Baseline Laminate	1.524 (0.06)	2.91 (85.5)
Thin Baseline with Polyurea coating	1.524 (0.06)	2.28 (67.4)

Experimental Methods

The experiments conducted in this study make use of a water filled tank coupled with high speed photography and Digital Image Correlation to impart UNDEX loading to fully clamped plates while capturing the transient response. The following are the details of the equipment and methods employed.

Test Tank

The near field UNDEX experiments in this study were conducted in a water filled tank, Fig. 3. The tank has internal dimensions of 1.21 m × 1.21 m × 1.21 m with 6.35 mm thick steel walls and is supported on a reinforced wooden stand. The tank contains ~1500 l of water when filled. Four window ports allow for the lighting and high speed photography of the UNDEX event and plate motion. Mounted to the inner surface of one wall is a 304.8 mm × 304.8 mm, rectangular tunnel with a wall thickness of 12.7 mm, which serves as the base for the mounting of the composite plates. The tunnel extends 394 mm into the tank from the wall and a 38.1 mm wide flange is welded to the end of the tunnel. The outer dimensions of the flange are 381 mm × 381 mm. The flange has a series of through holes around the perimeter which allow for bolting of the test plates to the flange. The test plates are sandwiched between the flange and a second steel frame and are secured to the flange with a series of 1.59 mm diameter through bolts spaced at 38.1 mm. The use of the tunnel and mounting flange provide a water tight seal around the test plate and allows for the plates to be air backed, Fig. 3.

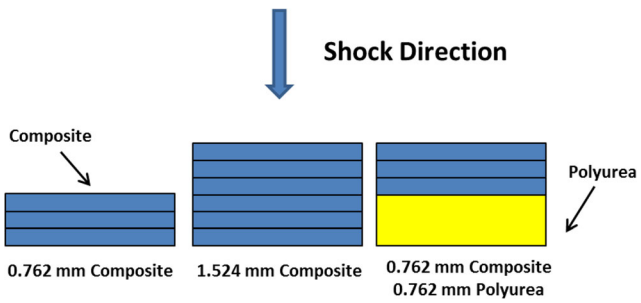

Fig. 2 Composite plate construction – Schematic (Not to scale)

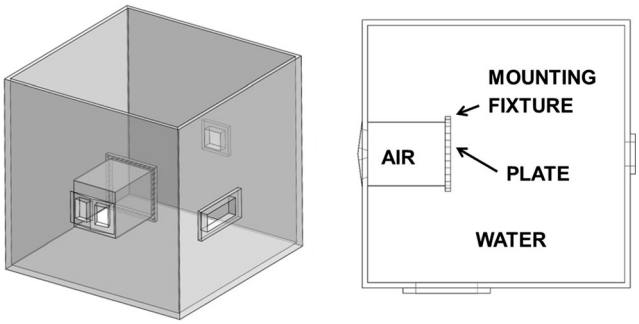

Fig. 3 UNDEX test tank

The composite plate and mounting fixture geometrical details are provided in Fig. 4.

Explosive Charge

The explosive used in the near field blast experiments is an RP-503 charge manufactured by Teledyne RISI, Fig. 5. The charge is comprised of 454 mg RDX and 167 mg PETN contained within an outer plastic sleeve.

Measurement Equipment

Pressure transducers / data recorder

The free field pressure transducers employed in this study to measure the pressure field resulting from the detonation of the RP-503 charge are Series 138 ICP Tourmaline Underwater Blast Sensors produced by PCB Piezotronics, Inc. (item number 138A05). The sensors have a pressure range of 34.475 MPa, rise time is less than 1.5 μs, and a resonant frequency greater than 1 MHz.

A Tektronix DPO 3034 Digital Phosphor Oscilloscope has been used to record the pressure histories during the near field blast experiments. The oscilloscope has 4 analog channels, each with a 2.5 GS/s sample rate, 300 MHz bandwidth, and 5 mega-point record length.

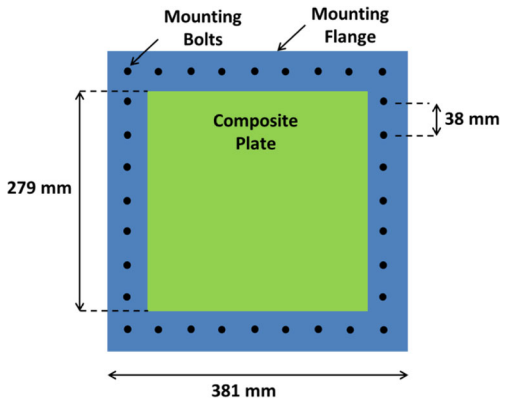

Fig. 4 Specimen geometry

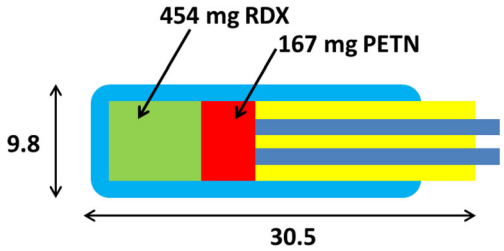

Fig. 5 RP-503 explosive charge (units of mm)

Digital image correlation

High speed photography, coupled with three dimensional Digital Image Correlation (DIC) was used to capture the full-field deformation of the back-face (side opposite of the explosive) of the plates during the UNDEX loading. During the experiments two cameras are arranged in a stereo configuration such that they view the back face of the test specimen. To record the transient response with this system, the cameras must be calibrated and have synchronized image recording throughout the event. The calibration of the cameras is performed by placing a grid containing a known pattern of points (dots) in the test space where the composite sample is located during the experiment. This grid is then translated and rotated in and out of plane while manually recording a series of images this grid pattern is predetermined, the coordinates of the center of each point (dot) is extracted from every image thus allowing for a correlation of the coordinate system of each camera. Prior to the conduct of the experiments, the face of the composite plate facing the cameras (back-face) is painted with a random speckle pattern (white background with small densely spaced black dots. The software employed to synchronize the high speed cameras and record the images during the experiments is Photron Fastcam Viewer (PFV). PFV is a user interface that enables the editing and storage of captured images and video. The post processing is performed with the VIC-3D software package which matches common pixel subsets of the random speckle pattern between the deformed and un-deformed images. The matching of pixel subsets is used to calculate the three-dimensional location of distinct points on the face of the plate. This provides a full-field displacement history of the transient event throughout time.

The cameras used during experimentation were Photron FastCam SA1. Each camera is capable of frame rates from 1,000 to 675,000 fps with image resolution ranging from 1,024×1,024 to 64×16 pixels depending on the frame rate. In the current effort, a frame rate of 27,000 fps was utilized for an inter-frame time of 37 μs. The camera resolution at this frame rate is 448×480 pixels.

Experimental Methodology

Experiments were preformed to understand the behavior of E-Glass/Epoxy plates subjected to near field underwater explosions. Three plate configurations have been studied: (1) 0.762 mm thick uncoated plate, (2) 1.524 mm thick uncoated plate, and (3) 0.762 mm thick plate with 0.762 mm polyurea coating on the back-face. Two high speed cameras were positioned 330 mm behind the tank walls perpendicular to the viewing windows to avoid any distortion effects from the windows themselves. A third high speed camera was positioned at the side of the tank to view the detonation of the explosive, resulting bubble growth, and interaction of the bubble with the composite plate. Two free field tourmaline pressure sensors are located within the tank to record the pressure field at two distinct standoff distances. Let it be noted that the gages are located at a larger standoff from the charge than the distance between the charge and the composite plate to avoid damage to the sensors. Figure 6 is a combination, isometric view and aerial schematic of the tank providing an overview of the camera, explosive and pressure sensor positioning. An overview of the experimental process is presented in the following discussion.

To begin the experiment, the high speed cameras comprising the DIC system are calibrated to establish a correspondence of the respective camera coordinate systems. Calibration is conducted according to the previously described method in which images of a calibration grid are captured while rotating and translating the grid. Once acceptable calibration and time syncing of the cameras is established the plate is bolted into the fixture with the DIC speckle pattern facing the cameras (air backed side). When mounting the polyurea coated plates, the coating is located on the back side of the composite plates with respect to the charge location. Once the plate is bolted into the fixture the RP-503 charge is placed within the tank. The charge is suspended by its detonation wire into the tank and placed 50.8 mm from the center of the composite plate. To ensure consistent charge standoff distances for each experiment a 3.18 mm diameter foam spacer is placed between the charge and plate. The foam is secured to both the charge and plate by a fast setting epoxy. The use of this foam spacer was critical to the conduct of the experiments for two reasons: (1) it ensures there is no disturbance of the charge location during the filling of the tank, and (2) it accounted for panel flexure (induced the hydrostatic load of the water after filling) by ensuring that the charge moved with the plate, thus maintaining a consistent standoff distance. Two tourmaline pressure sensors are positioned in the tank at horizontal standoff distances from the charge center of approximately 100 and 175 mm. The sensors are suspended in the tank from their water resistant cables and are also secured to a weight on the bottom of the tank by means of a thin line to maintain relative positioning. Each sensor is then fixed in position by a wire which is secured to a weight resting on the bottom of the tank. After the plate is secured in the fixture and the pressure sensors are in place, the tank is filled with water to a depth of 1.06 m. The center of the plate is located 0.55 m below the surface of the water. As mentioned previously, an aerial schematic of the total setup is shown in Fig. 6.

Once the tank is filled, and the operation of all measurement equipment is verified, the RP-503 charge is detonated through the use of a detonation box. The box simultaneously sends a high voltage to the RP-503 charge to initiate detonation and a simultaneous 9 V pulse to the oscilloscope which captures the pressure data. The oscilloscope also relays a negative TTL voltage to all the cameras to capture the high speed photos. The use of this single initiation system to both initiate

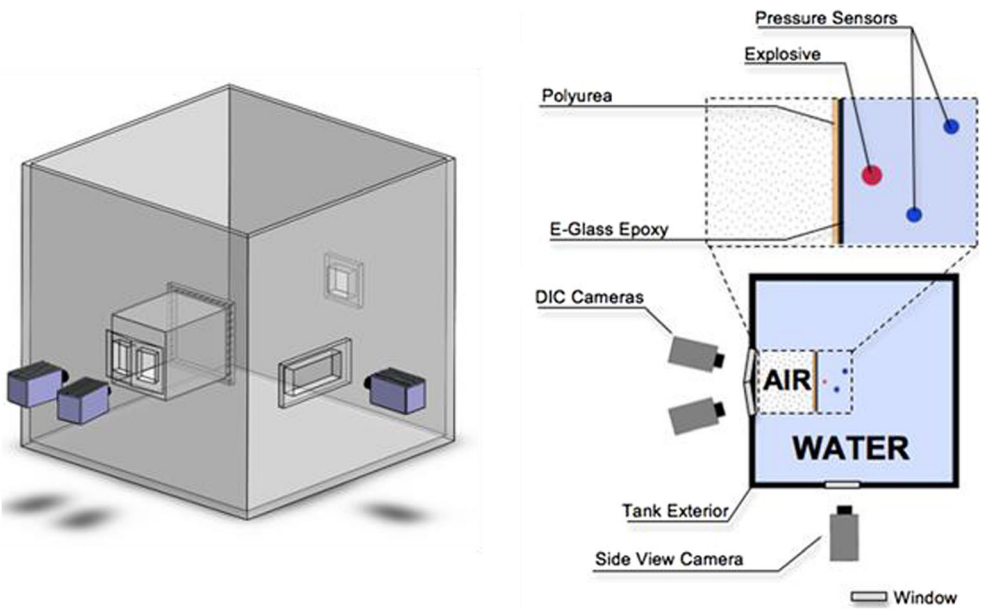

Fig. 6 Experimental setup measurement equipment

the charge detonation and trigger the oscilloscope/cameras ensures complete time synchronization between all experimental equipment and a common time zero datum for all measurements. Upon completion of the experiment all images from the DIC cameras are processed through VIC 3D to extract full-field plate deformation.

Results and Discussion

The response of the composite plates in this study is characterized by the transient center-point displacement of the backface of the plate, deformation evolution mechanisms during the displacement, and full-field DIC observations. All plate deflection data presented for the plates is extracted from the post processed images through DIC.

The pressure profiles resulting from the detonation of the RP-503 charge, as measured by the two free field pressure sensors at 100 and 175 mm standoff distances from the charge, are shown in Fig. 7. The pressure profiles display the characteristic components of an UNDEX, namely: a rapid pressure increase associated with the shock front, followed by an exponential decay and a reduction in peak pressure with increasing radial standoff from the charge center. It is noted that for the 100 mm standoff pressure gage there is a sudden drop in pressure occurring at 0.12 ms. This corresponds to the arrival of the reflected pressure wave from the surface of the plate. The peak pressure of the shock front experienced by the plate surface (50.8 mm standoff) is on the order of 40 MPa determined from the computational simulations.

The behavior of the bubble resulting from the detonation and its associated interaction with the composite plate is shown in Fig. 8. The sequence of images shows the clear formation of the bubble at 80 μs and its subsequent growth in size due to the combustion of the explosive products. Due to the high pressure of these gaseous products the bubble expands, reaching a diameter of ~50 mm at 320 μs at which point it reaches and

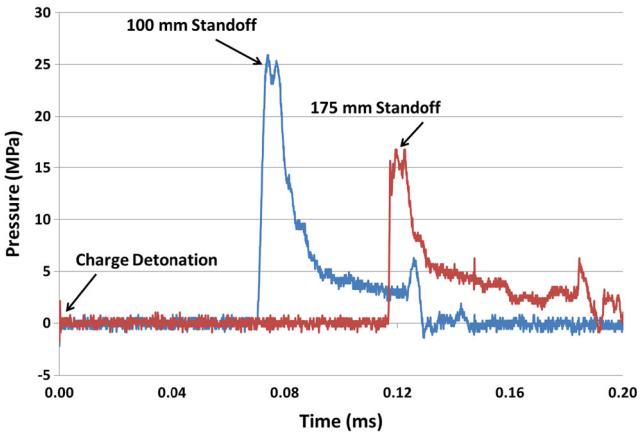

Fig. 7 UNDEX pressure profiles (Time zero corresponds to charge detonation)

interacts with the surface of the composite plate. As a result of this interaction with the plate it is prevented from further expansion in the direction of the plate but continues a spherical expansion in the remaining directions. The uncoated plates experience edge tearing (see later discussion) between 1200 μs and 1400 μs during which time the bubble is still expanding and has not yet reached its maximum diameter. Once tearing of the plate occurs, the plate can no longer be considered a standing plate and any resulting bubble behavior would be heavily influenced by the resulting motion of the plate. Figure 8 displays only the first 560 μs of the bubble behavior to show initial plate contact and radial expansion. Times between 560 and 1200 μs consist mainly of further bubble expansion, thus images after 560 μs are not shown.

While filing tank with water during the setup of the experiment it was observed that the plates sustain a measurable level of flexure due to the hydrostatic pressure and the thin nature of the plates. The peak center-point deflection of the plates after filling the tank is provided in Table 3. These deflections are determined by taking photographs of the plate surface before and after filling the tank and processing the images through the DIC software. The baseline for all subsequent plate deflection measurements is taken to be the deformed shape after tank filling. As previously described, a constant charge standoff for all plate configurations is achieved through the use of a foam spacer which connects the charge and plate. Although beyond the scope of the current study, it is noted that it is likely that as the initial depth pressure is increased (i.e., a deep diving submersible) the effects of the corresponding pre-stress prior to UNDEX loading should be considered. As the material has a finite strength capability, the additive effect of depth pressure and UNDEX pressure loading will reduce the ability of a structure to resist an explosion event that may have been survivable at shallower depths.

The center-point displacement for each respective plate configuration is shown in Fig. 9. From this figure it is observed that there are several distinct differences in the overall plate response as influenced by the plate construction. The first difference is the overall center-point deflection of the plates. It is evident that, as compared to the baseline 0.762 mm plate, increasing the plate thickness or including a polyurea coating reduces the peak overall deflection for a given level of loading. The peak displacement for the uncoated 0.762 mm plate is 28 mm, whereas for the 1.524 mm uncoated plate and the 0.762 mm polyurea coated plate the peak deflections are 20.5 mm and 24.8 mm, reductions of 27 and 12 % respectively. It is noted that the center-point velocity during the initial deflection is nearly constant for each configuration. The main difference is the time that it takes for the plate to arrest its outward motion and begin to recover, with the 1.524 mm uncoated and the 0.762 mm polyurea coated plates arresting their outward motion ~0.25 ms sooner than the baseline 0.762 mm plate. The peak center-point deflection and time to reach the

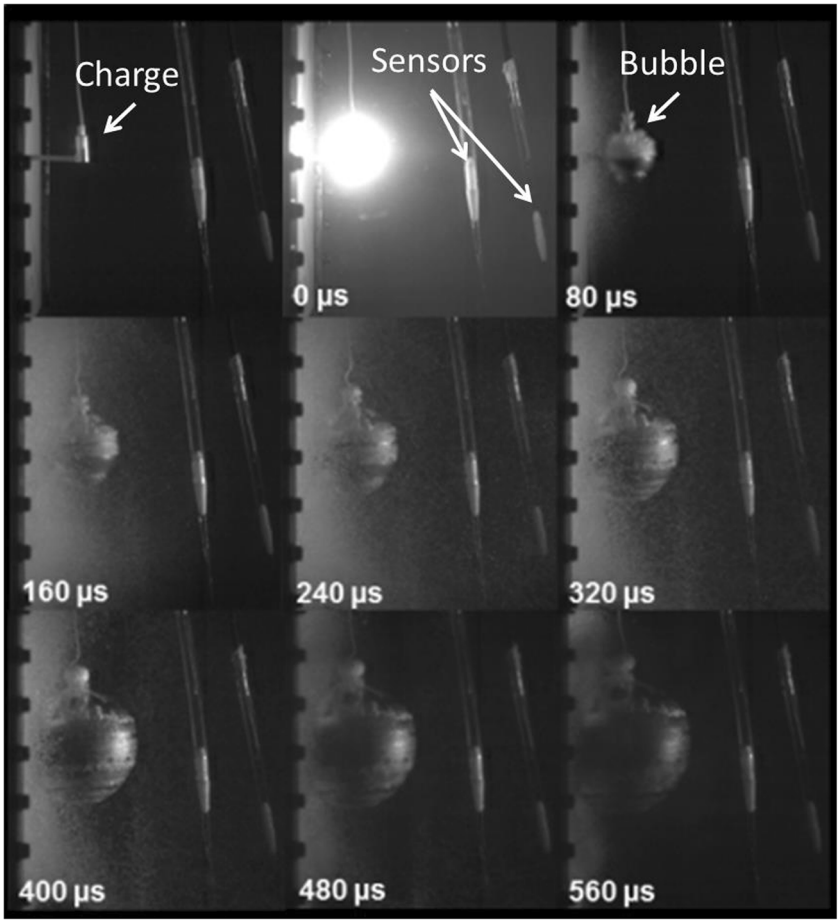

Fig. 8 UNDEX gas bubble behavior

peak displacement are provided in Table 4. The center-point deflection comparison between the 1.524 mm uncoated plate and the 0.762 mm plate with a 0.762 mm coating of polyurea indicate that for a plate thickness it is more advantageous to utilize additional structural plies rather than an elastomeric coating. However, when a structure has previously been designed and further thickening of the structural shape is not possible, the application of a polyurea coating can improve the transient response to shock loading.

The second primary difference in the response of the plate configurations is the onset of material damage. Both the uncoated 0.762 and 1.524 mm specimens experienced significant through-thickness tearing at the plate boundaries at approximately 1.1 and 1.4 msec respectively. Upon rupture of the plate edges water entered the cameras' field of view and caused decorrelation in the DIC images. Their plots, Fig. 9, are accordingly abbreviated at the onset of tearing prior to DIC decorrelation due to water instrusion. However, it is further observed that although the 0.762 mm plate with the polyurea coating did experience larger deflections than the 1.524 mm uncoated plate, there was no edge tearing of the plate itself. Thus in terms of reducing material damage itself, the polyurea coatings offer an advantage over a thicker uncoated plate.

Table 3 Specimen deflections under hydrostatic preload

Plate	Deflection (mm)
0.762 mm (Uncoated)	5.6
0.762 mm (Coated)	5.3
1.524 mm (Uncoated)	4.6

The deformation history of the baseline 0.762 mm uncoated composite plate as measured along a horizontal cut though

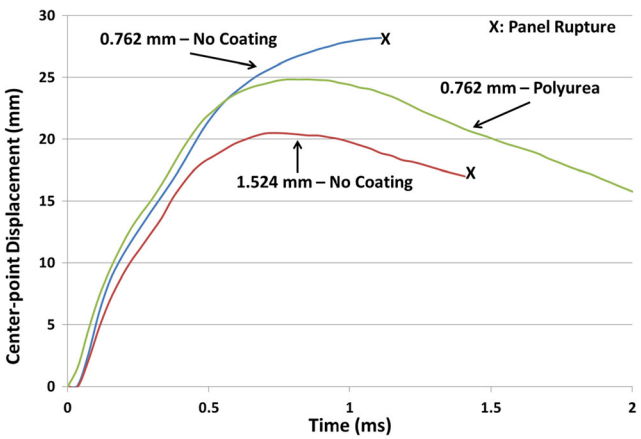

Fig. 9 Plate center-point deflections

Table 4 Plate center-point deflection results

Plate	Maximum deflection	Time to peak
0.762 mm (Uncoated)	28.2 mm	1.07 msec
0.762 mm (Coated)	24.8 mm	0.78 msec
1.524 mm (Uncoated)	20.5 mm	0.74 msec

the center of the plate is shown in Fig. 10. The deformed profile plotted throughout time is illustrative of the deformation mechanics of the composite plate. From this figure it is seen that for a plate subjected to a centralized near field UNDEX loading, the deformation is initially dominated by localized deflections at the center with minimal deflection near the boundaries. As the plate responds to the pressure loading, it gradually transitions to an overall plate flexure mode as shown by the cross sectional shape at 0.63 and 1.11 ms. At 1.11 ms the plate experiences significant edge tearing and further observations of the plate deformation mechanics would be invalid due to partial rigid body motion of the plate. The significant observation is that the initial plate deformation is governed by the highly localized pressure loading and then subsequently shifts to a mode I flexure deformation profile later in time.

The full-field displacement profiles for the back-face of each plate configuration are provided in Fig. 11. The localized center-point deflection can be visualized in the 0.37 ms time frame and is consistent with the cross sectional shape plot, Fig. 10. Furthermore the overall flexural deformation mode at 1.11 ms is clearly visible in the contour plots. Each of the three panel configurations exhibit similar deformation along their centerline with the primary difference being the magnitude of the displacement itself.

The transient displacement results discussed thus far indicate a performance advantage when the thickness of the baseline plate is increased, or alternatively a polyurea coating is applied to the surface of the plate. However, when the plate thickness is increased or a coating is applied there is an

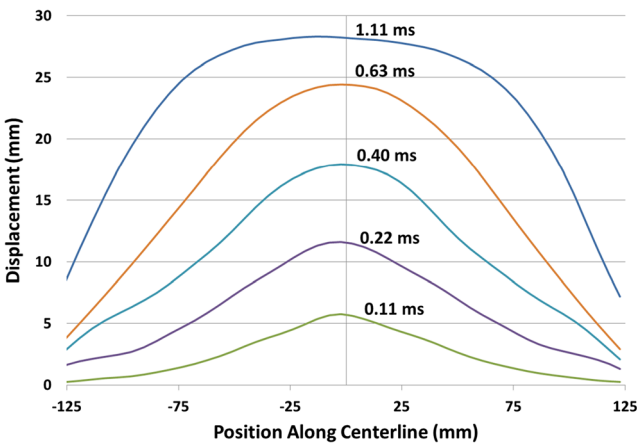

Fig. 10 Plate deformation - horizontal centerline

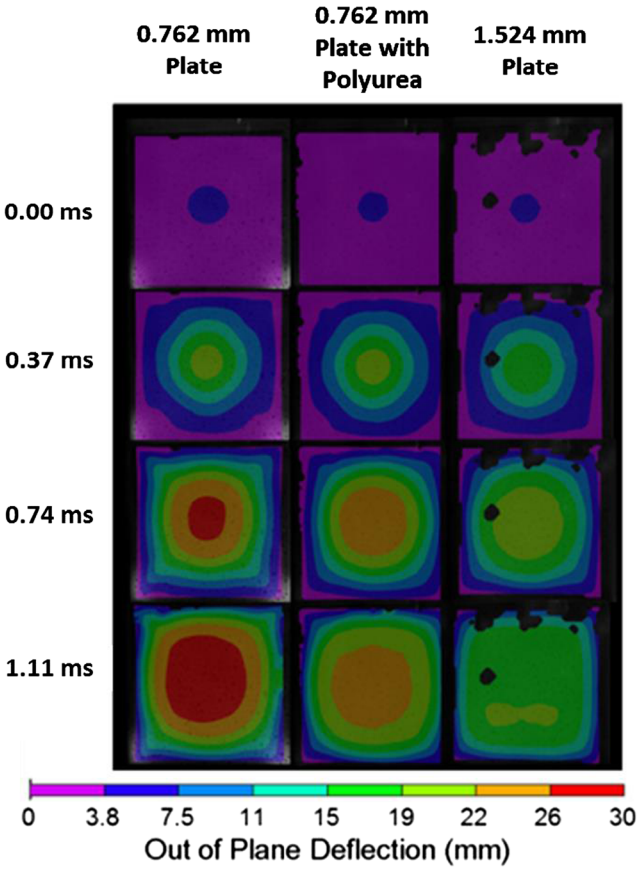

Fig. 11 Full-field deflection contours

associated penalty in that the plate weight is correspondingly increased. One means of quantifying the added mass penalty in terms of transient deflection of the respective plates is to establish an Areal Weight Ratio (AWR) between the plate configurations [13]. The AWR is calculated by (equation (1))

$$AWR = \frac{W_{2,3}}{W_1} \tag{1}$$

where W_1 is the areal weight of the uncoated 0.762 mm composite baseline plate and $W_{2,3}$ is the areal weight of the polyurea coated 0.762 mm plate and the and 1.524 mm specimens, respectively. The AWRs for the 1.524 mm plate and the polyurea coated plate are 2 and 1.57 (Table 2). The AWR is subsequently employed as a multiplier applied to the transient center-point deflection data. The displacement data that has been adjusted (raw data multiplied by AWR) to account for the areal mass increase is shown in Fig. 12. This plot shows that when the displacements are adjusted to account for the increased areal weight, the baseline plate outperforms both the thicker and polyurea coated plates. The normalized deflection of the polyurea coated specimen was 37.9 % greater than the uncoated 0.762 mm specimen, and that the normalized deflection of 1.524 mm specimen was similarly 45.4 % greater. This suggests that the additional laminate plies and the employed

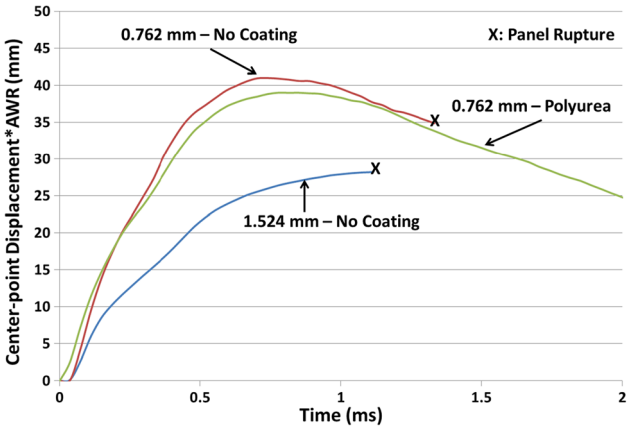

Fig. 12 Areal weight adjusted deflections

polyurea regime serve to degrade the deflection performance of the plate specimen with respect to AWR. This observation is consistent with previous findings for curved polyurea composite plates subjected to far field UNDEX loading in which polyurea coatings have been seen to result in larger AWR adjusted deflections [13]. It is noted that in the previous study, multiple coating thicknesses were considered and it was found that there are coating thicknesses for which the coated plate outperforms the baseline plate, even when accounting for the AWR penalty. Thus, the findings of the single coating thickness considered in the current study do not preclude the existence of a polyurea coating thickness for composite plates subjected to near field UNDEX loading that both outweighs the weight penalty while also improving the deflection performance. Further work is needed to identify such a regime in the future. Finally, the 1.524 mm plate and 0.762 mm polyurea coated plates have approximately the same relative performance in terms of adjusted peak displacement when the added mass penalty is taken into consideration (Table 5).

Finite Element Modeling

Finite element modeling of the experiments has been performed with the LS-DYNA code available from the Livermore Software Technology Corporation (LSTC). The models utilize the coupled Lagrange-Eulerian formulation of the code which allows for accurate representation of the detonation of the explosive charge as well as the fluid structure interaction between the fluid and the composite plate. All simulations are generated with Version 971, Release 4.2.1 and are run in double precision mode. All models are constructed in the CGS unit system.

Table 5 Normalized plate center-point deflection results

Plate	Maximum AWR deflection
0.762 mm (Uncoated)	28.2 mm
0.762 mm (Coated)	38.9 mm
1.524 mm (Uncoated)	41.0 mm

The finite element model of the UNDEX test setup is shown in Fig. 13. The model consists of the test plate (Coated / Uncoated Composite Plate), tank water, air, and the RP-503 charge. The model represents a subdomain of the full experimental test tank for computational efficiency. Included in the model is the unsupported portion of the composite plate (Plate edge corresponds to the clamped boundary), 120 mm of air extending behind the plate, and 200 mm of water extending from the plate surface towards the charge. The charge is located 50.8 mm from the center of the plate surface. The use of such a sub-domain for the modeling of the corresponding experiments is deemed appropriate as the loading of the plate and subsequent response occurs sufficiently fast that reflections from the tank walls do not affect the overall transient response of the plate. In the model the outer surface of the fluid sub-domain is prescribed a non-reflecting boundary condition (*BOUNDARY_NON_REFLECTING) which allows the associated pressure waves to leave the domain, as they would in a free field detonation, rather than reflect off of the free surface.

The water, air, and explosive charge are modeled with solid elements utilizing the LS-Dyna ALE multi-material element formulation (Type 11 solid element). Each of the Eulerian components in the model utilizes a material definition in combination with an equation of state (EOS) to fully define the appropriate behavior. The water and air utilize the *Mat_Null material definition with the density of the water and air given as 1 g/cm^3 and 0.0013 g/cm^3 respectively. The Gruneisen EOS is used for the definition of the water with the speed of sound taken to be 149,000 cm/s. A Linear Polynomial EOS defines the air domain in the model with the parameters defined in Table 6. By defining C_0, C_1, C_2, C_3, and C_6 equal to zero, and C_4, and C_5 equal to γ-1, a gamma law EOS is achieved. Finally, the explosive charge is modeled with the *Mat_High_Explosive_Burn material model combined with the JWL EOS. Although the RP-503 charge contains both RDX (454 mg) and PETN (167 mg), the model assumes a charge comprised of only RDX, with the overall charge weight being maintained. This is deemed suitable for the model since the RDX is the larger component and RDX and PETN have similar JWL coefficients. Furthermore, the pressure generated from the detonation in the model is suitably correlated to the corresponding experimental profile. The Material and EOS parameters for the RDX are provided in Tables 7 and 8.

The structural aspect of the coupled model consists of the composite plate and polyurea coating. In all models, only the unsupported section of the plates is included. The outer edge of the plate is fully clamped with appropriate boundary conditions, thus negating the need to explicitly model the fixturing in the test setup. It is noted that after the completion

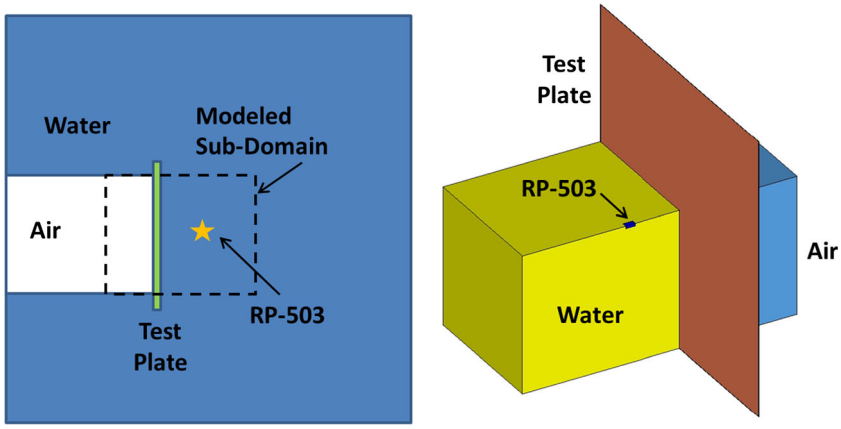

Fig. 13 Finite element model of UNDEX experiment (3 quadrants of fluid domain hidden)

of each test there was no slippage observed at the plate boundary. The composite plate in the simulations is modeled using a single layer of shell elements, Fig. 14, with an edge length of 2.5 mm. The *Section_Shell property for the shell element allows for the laminate schedule to be defined within the section card, including the angle of each respective ply. By defining the ICOMP parameter to be equal to 1 on the section card, the orthotropic layered composite option is activated. Through the use of this option an arbitrary number of equally distributed integration points may be defined through the thickness of the shell, with each integration point being assigned a material angle. In the current models, each ply is represented as having two integration points so as to capture the correct bending behavior on a per ply level. The polyurea material is represented in the model by solid elements, Fig. 14, with a constant stress formulation. Furthermore, the polyurea coatings are assumed to be perfectly bonded to the composite plate and are thus meshed directly to the composite. This assumption is valid as there was no visual de-bonding between the composite and polyurea observed during testing.

The LS-DYNA material model utilized for the composite plate is Mat_Composite_Damage (Mat_022) [20]. This is an orthotropic material definition capable of modeling the progressive failure of the material due to any of several failure criterions including in-plane shear, tension in the longitudinal/transverse directions, and compression transverse direction. The input material properties are those provided in

Table 1. The material model for the polyurea coating is Mat_Simplified_Rubber. This model is a visco-elastic material definition which captures both the strain and strain-rate effects through the use of a family of load curves. The model reproduces the uniaxial tension and compression behavior as obtained through material testing at discreet strain rates. The stress–strain curves for each strain rate are shown in Fig. 1. The model determines the appropriate strain rate curve from the family of curves through an internal calculation.

The loading of the composite plates in the models occurs in a two-step process. During the first step a uniform pressure is quasi-statically applied over the entire front face of the plate. This pressure corresponds to the depth pressure (at the mid point of the plate) acting on the submerged plate. During the experiments it was observed that due to the relatively thin nature of the plates as compared to the unsupported dimensions of the plate there was a sufficient level of center-point defection (~5 mm for all plates) such that it should be accounted for during the simulations. Thus this pressure is applied to the plates and any resulting motion is allowed to damp out resulting in a static stress state. At this point the detonation of the explosive charge is initiated and the plate responds transiently. In all subsequent discussions of plate displacements, the reported values are measured from the preloaded state by subtracting out the displacement resulting from the preload.

Table 6 Air EOS parameters

C0	0
C1	0
C2	0
C3	0
C4	0.4
C5	0.4
C6	0

Finite Element Model Correlation to Test Data

Center-point Displacement – Simulation Correlation to Test

The center-point displacement data captured during the experiments with the DIC method is used as a basis to correlate and validate the finite element model results. The quality of the

Table 7 RDX material parameters

ρ (g/cm^3)	1.77
D (cm/s)	850e3
Chapman-Jouget Pressure (dyn/cm^2)	3.41e13

Table 8 RDX EOS (JWL) parameters [19]

A	7.78e12 (dyn/cm^2)
B	7.07e10 (dyn/cm^2)
R1	4.485
R2	1.068
ω	0.3
E_o	5.93e10
V_o	1.0

correlation between the test data and numerical results in this study is quantified using the Russell Comprehensive Error measurement. The Russell error technique is one method which evaluates the differences in two transient data sets by quantifying the variation in magnitude and phase. The magnitude and phase error are then combined into a single error measure, the comprehensive error factor. The full derivation of the error measure is provided by Russell [21] with the phase, magnitude, and comprehensive error measures respectively given as:

$$RP = \frac{1}{\pi}\cos^{-1}\left(\frac{\sum c_i m_i}{\sqrt{\sum c_i^2 \sum m_i^2}}\right)$$

$$RM = sign(m)\log_{10}(1+|m|)$$

$$RC = \sqrt{\frac{\pi}{4}\left(RM^2 + RP^2\right)}$$

In the above equations c_i and m_i represent the calculated (simulated) and measured responses respectively. Excellent, acceptable, and poor correlation using the Russell error measure is given as: Excellent - RC≤0.15, Acceptable – 0.15< RC≤0.28, and Poor RC>0.28. The definition of these criteria levels are the result of a study that was undertaken to determine the correlation opinions of a team in support of a ship shock trial. A summary of the process used to determine the criteria is presented by Russell [22].

The center-point time history correlation between the experimental data and the corresponding computational simulation for each respective plate configuration is shown in Fig. 15. A summary of the Russell error for each of these comparisons is provided in Table 9. The correlations presented in the figure show that there is a high level of correlation between the experiment and simulations, both temporally and in terms of displacement magnitudes. The simulation and experiment results exhibit consistent results in the early time frame of the event (0 – 0.4 ms) in terms of displacement and velocity, with some deviation beyond this point, although the deviation is somewhat minor. Additionally for both of the

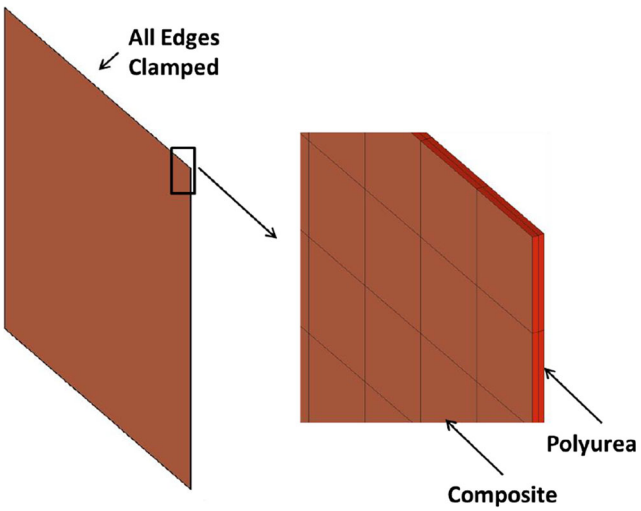

Fig. 14 Structure mesh details

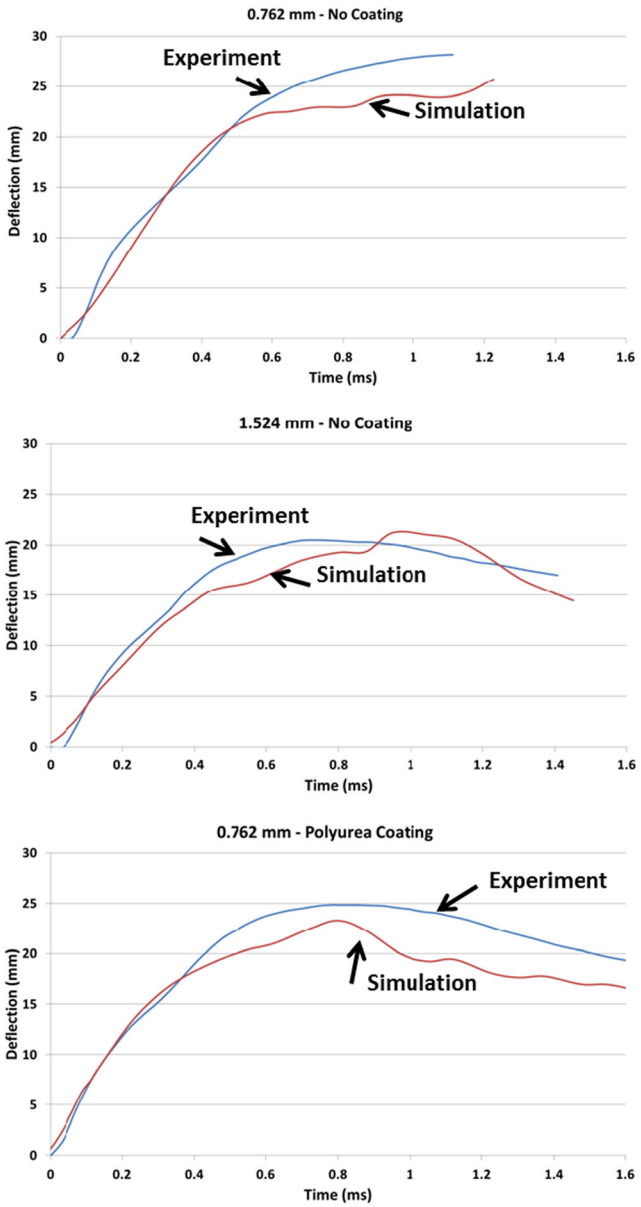

Fig. 15 Center-point displacement model correlation

Table 9 Russell error measure summary

	Magnitude error (RM)	Phase error (RP)	Comprehensive error (RC)
0.762 mm (Uncoated)	0.08	0.02	0.07
0.762 mm (Coated)	0.10	0.02	0.09
1.524 mm (Uncoated)	0.03	0.02	0.03

RC<0.15 – Excellent

0.15<RC<0.28 – Acceptable

RC>0.28 - Poor

uncoated plates (0.762 and 1.524 mm) it is seen that the onset of edge tearing occurs slightly later (0.1 ms) in time as compared to the experimental results. The timing differences in the onset of damage is expected as the model assumes a uniform plate in terms of material properties and does not account for manufacturing variability or minor internal defects which can contribute to the onset of damage or slightly weaker/stronger areas of the plates as compared to the gross material strengths. That the model is able to predict the onset of damage in a consistent manner as observed during the testing, namely edge tearing, is encouraging. Overall, it is shown that the Russell error values for the center-point comparisons show excellent correlation (RC<0.15).

Summary and Conclusions

The response of submerged, air backed E-Glass / Epoxy composite plates, including polyurea coatings, when subjected to near field underwater explosive loading has been studied through the use of experiments and computational modeling. The focus of the work is on determining how the response of a composite plate subjected to UNDEX is influenced by increased plate thickness or through the application of an elastomeric coating to the baseline plate. A water filled blast tank has been used to impart UNDEX loading to the composite plates in a controlled manner. The Digital Image Correlation system is used to capture the full-field, transient response of the back (dry) surface of the plates. Computational models of the experiments have been developed utilizing the commercially available LS-DYNA explicit finite element code.

In the study the response of three unique plate configurations is studied: (1) 0.762 mm baseline plate, (2) 1.524 mm plate, and (3) 0.762 mm plate with a 0.762 mm polyurea coating applied to the back-face. Performance of the plate configurations is evaluated using the center-point and full-field time histories of the deflection of the back-face of the plates, as well as level of material damage. The experimental results show several effects on the transient response of the plates based on configuration. The use of a plate two times as thick as the baseline plate reduces the center-point defection by 27 % while the application of a polyurea coating equal in thickness to the baseline plate results in a 12 % deflection decrease. Additionally, the polyurea coating is effective in reducing material damage as compared to both the baseline and thicker uncoated plates. Thus, when considering a plate design, the desired performance metric of the plate response should be considered. A thicker plate of structural material (composite) is preferable to reduce center-point deflection, while the use of polyurea coating are effective in reducing overall damage. However, in the case of an existing design the use of polyurea coatings can be an effective retrofitting application to improve the blast resistance of a structure while reducing overall material damage. Furthermore, it has been shown that through the use of an Areal Weight Ratio, there is a tradeoff between increased panel weight and mechanical performance. Although, both the thicker composite plate and the coated plate outperform the baseline plate, this performance increase comes at a penalty of increased weight. Thus if weight is a strong consideration in a specific application then maximum blast resistance may not be achievable and a relative tradeoff between weight and performance must be considered. The computational models developed in the study to correspond to the experimental testing, simulate the testing accurately, and using the Russell Error measure, demonstrate model correlation that can be described as excellent. The models are able to accurately simulate the detonation of the explosive charge and the resulting pressure fields and plate deflections.

Acknowledgments The financial support of the Naval Undersea Warfare Center (Division Newport) In-house Laboratory Independent Research program (ILIR) directed by Neil Dubois is greatly acknowledged. The support of Dr. Y.D.S. Rajapakse of the Office of Naval Research under Grant Nos. N00014-10-1-0662 (University of Rhode Island) and N00014-14-WX00730 (Naval Undersea Warfare Center, Division Newport)) is acknowledged.

References

1. Latourte F, Gregoire D, Zenkert D, Wei X, Espinosa H (2011) Failure mechanisms in composite plates subjected to underwater impulsive loads. J Mech Phys Solids 59:1623–1646
2. Espinosa H, Lee S, Moldovan N (2006) A novel fluid structure interaction experiment to investigate deformation of structural elements subjected to impulsive loading. Exp Mech 46(6):805–824
3. Schiffer A, Tagarielli V (2015) The Response of circular composite plates to underwater blast: experiments and modeling. J Fluids Struct 52:130–144
4. Avachat S, Zhou M (2014) Response of cylindrical composite structures to underwater impulsive loading. Procedia Eng 88:69–76
5. Avachat S, Zhou M (2015) High-speed digital imaging and computational modeling of dynamic failure in composite structures subjected to underwater impulsive loads. Int J Impact Eng 77:147–165
6. LeBlanc J, Shukla A (2010) Dynamic response and damage evolution in composite materials subjected to underwater explosive

loading: an experimental and computational study. Compos Struct 92:2421–2430
7. LeBlanc J, Shukla A (2011) Dynamic Response of curved composite plates to underwater explosive loading: experimental and computational comparisons. Compos Struct 93:3072–3081
8. Franz T, Nurick G, Perry M (2002) Experimental investigation into the response of chopped-strand mat glassfibre laminates to blast loading. Int J Impact Loading 27:639–667
9. Mouritz AP (1995) The effect of underwater explosion shock loading on the fatigue behaviour of GRP laminates. Composites 26:3–9
10. Dear J, Brow S (2003) Impact damage processes in reinforced polymeric materials. Compos A: Appl Sci Manuf 34:411–420
11. Hodge N (2004) Military experimenting with 'Spray On' armor for humvees. Defense Today 25
12. LeBlanc J, Shukla A (2015) Response of polyurea coated flat composite plates to underwater explosive loading. J Compos Mater Article in Press doi:10.1177/0021998314528263
13. LeBlanc J, Gardner N, Shukla A (2013) Effect of polyurea coatings on the response of curved e-glass / vinyl ester composite plates to underwater explosive loading. Compos Part B 44:565–574
14. Tekalur SA, Shukla A, Shivakumar K (2008) Blast resistance of polyurea based layered composite materials. Compos Struct 84: 271–281
15. Gardner N, Wang E, Kumar P, Shukla A (2012) Blast mitigation in a sandwich composite using graded core and polyurea interlayer. Exp Mech 52:119–133
16. Amirkhizi A, Isaacs J, McGee J, Nemat-Nasser S (2006) An experimentally-based viscoelastic constituitve model for polyurea, including pressure and temperature effects. Phil Mag 86:5847–5866
17. Amini MR, Isaacs JB, Nemat-Nasser S (2010) Experimental investigation of response of monolithic and bilayer plates to impulsive loads. Int J Impact Eng 37:82–89
18. Amini MR, Simon J, Nemat-Nasser S (2010) Numerical modeling of effect of polyurea on response of steel plates to impulsive loads in direct pressure-pulse experiments. Mech Mater 42:615–627
19. Dobratz B (1972) Properties of chemical explosives and explosive simulants. Lawrence Livermore National Laboratory
20. LS-DYNA Keyword Users Manual – Volume II material models, livermore software technology corporation, May 2015
21. Russell DM (1997) Error measures for comparing transient data, Part I: development of a comprehensive error measure, Part II: error measures case study. Proceedings of the 68th Shock and Vibration Symposium 3–6
22. Russell DM (1998) DDG53 Shock trial simulation acceptance criteria. 69th Shock and Vibration Symposium 12–19